Ouyang *et al.*
*Protection and Control of Modern Power Systems* (2023) 8:12
https://doi.org/10.1186/s41601-023-00283-0

Protection and Control of Modern Power Systems

ORIGINAL RESEARCH

Open Access

# Coordination control method to block cascading failure of a renewable generation power system under line dynamic security

Jinxin Ouyang[1*], Jianfeng Yu[1], Xiaoxuan Long[2], Yanbo Diao[3] and Jian Wang[1]

**Abstract**

The large application of renewable energy generation (REG) has increased the risk of cascading failures in the power system. At the same time REG also provides the possibility of new approaches for the suppression of such failures. However, the capacity and position of the synchronous generator (SG) involved in regulation limit the power regulation speed (PRS) of REG to the overload line which is the main cause of cascading failures, while the PRS of SG is related to the position and shedding power. REG and SGs have difficulty in achieving effective cooperation under constraints of system power balance. Particularly, the dynamic variation of line flow during power regulation causes new problems for the accurate evaluation of line thermal safety under overload. Therefore, a new strategy for quantitatively coordinating shedding power and power regulation to block cascading failures in the dynamic security domain is proposed in this paper. The control capability and dynamic security domain of the overload line are modeled, and the coordination control method based on power regulation is then proposed to minimize shedding power. The algorithm for the optimal control scheme considers the constraints of load capacity, power source capacity and bus PRS. The correctness of the proposed method is verified using case studies.

**Keywords** Cascading failures, Overload, Shedding power, Power regulation, Thermal stability

## 1 Introduction

The application of renewable energy generation (REG) in power systems has progressed considerably. Large-scale construction of REG significantly increases the complexity of power systems and the risk of cascading failures intensifies rapidly. Consequently, highly efficient controls are required for safe operation [1, 2]. Doubly-fed and direct-driven wind turbines, and photovoltaic systems with power electronic interfacing elements are the main types of equipment of REG [3–5]. Power electronic elements enable the flexible power control capability of REG [6], e.g., REG can realize power reduction by pitch angle control, over-speed control and increasing working voltage, etc. Thus, the flexible power control of REG can provide a new solution for blocking cascading failures.

Line overload occurs when the line current exceeds the allowable long-term operating current and is the main cause of the cascading failures [7–9]. The power flow transfer caused by the outage of a faulty component can easily generate line overload under the impact of severe weather and high-load operation. The line temperature continues to rise after the overload, and short-circuit faults due to the increased sag or line damage from thermal oxidation can occur when the line temperature exceeds the maximum allowable value [10]. Therefore, relay protection is used to trip the overload line when required. However, the aggravated transfer of power flow

*Correspondence:
Jinxin Ouyang
jinxinoy@163.com
[1] State Key Laboratory of Power Transmission Equipment and System Security and New Technology, School of Electrical Engineering, Chongqing University, Chongqing, China
[2] Information and Communication Branch of State Grid, Chongqing Electric Power Company, Chongqing, China
[3] Chongqing City Management College, Chongqing, China

and line tripping after the protection action may cause cascading failures.

Some studies deal with the attempt to avoid cascading failures by improving the protection principle and setting [11, 12]. However, these methods can only delay the line tripping to provide additional time for emergency control, but cannot completely avoid the line tripping or withdrawal of a large number of components after line tripping. Thus, blocking cascading failures is generally challenging. Temperature rise is the primary cause of line tripping and cascading failures, though line heating is a slow process. If the line current can be decreased to a value below the long-term allowable current in the allowable overload time, then line overheating can be prevented and line tripping avoided. Therefore, the line flow should be decreased to ensure the safe recovery of the overload line so as to block cascading failures [13].

Generator tripping and load shedding can reduce line flow directly [14]. However, shedding power may cause reliability problems, economic losses, and even stability problems [15]. Regulating the power of generators to gradually reduce the line flow is an effective method [16], but the safe recovery of the overload line cannot be achieved solely with a synchronous generator (SG) because of restricted power regulation speed (PRS). Applications of the power control capability of REG in power system operation have attracted considerable research attention. Some studies have proposed the coordination of generator tripping, load shedding and power regulation to reduce the current of the overload line in the optimization method. However, cost was the main objective for coordination while the consequences and effects caused by generator tripping on the power regulation ability were neglected.

The security boundary of line overload is the basis of coordination control. Reducing the current to the long-term allowable value within the allowable overload time is a widely used method [17]. The allowable overload time depends on heating and heat dissipation power values [18]. The line current mainly determines the heating power while the environment and line temperature affect the heat dissipation power. The allowable overload time then must be dynamic during the power regulation because of the change of line flow. However, the influence of power variation is ignored in existing studies, and the allowable overload time is treated as a constant value and this inevitably causes significant errors in power regulation [16]. Some studies allow that the allowable overload time is variable, but only the different initial overload power is considered [19]. Neglecting the dynamic characteristics of the allowable overload time can increase operating costs and cause line damage or even cascading failures because of insufficient control.

A new method for blocking cascading failures by coordinating the generator tripping, load shedding and power regulation of SG and REG, on the basis of the dynamic security domain of line, is proposed in this study. The influence of initial overload power, mutation power, and continuous power regulation on line security is described. The accurate evaluation of dynamic security is realized by modeling the power control capability of the overload line.

Quantitative coordination control is realized with consideration of the interaction between the amount and position of shedding power and the PRS of SG and REG, by modeling the dynamic security domain of the overload line. Damage to or tripping of the line can be effectively avoided with the maximum use of power regulation capability while minimizing the shedding power. Therefore, cascading failures can be effectively blocked.

The remainder of this paper is organized as follows. The control capability of the overload line is characterized by modeling the power regulation capabilities of SG and REG in Sect. 2. The method for evaluating the dynamic security of the overload line via mutation power and integrated PRS is proposed in Sect. 3, while the principle of coordination control is put forward in Sect. 4. The producing algorithm of the optimal control scheme considering the constraints of load capacity, power source capacity and bus PRS is discussed in Sect. 5. The proposed method is verified using case studies in Sect. 6, and conclusions are drawn in Sect. 7.

## 2 Modeling of control capability of overload line

Generator tripping, which is generally matched with load shedding, can reduce line flow but cause system power mutation [20]. The shedding power of generator buses must be less than its initial power and important loads should be guaranteed. Therefore, the shedding power should be less than the difference between its initial power and important loads. The PRS of a SG is limited because of the inertia in the rotor, while the power output of a SG cannot be excessively small because combustion should be maintained. Therefore, the power regulation capability of a SG can be modeled as:

$$\begin{cases} -R_{si\mathrm{d}}\Delta t \le \Delta P_{si} \le R_{si\mathrm{u}}\Delta t \\ P_{si,\mathrm{mi}} < \Delta P_{si} + P_{si0} < P_{si,\mathrm{ma}} \end{cases} \tag{1}$$

where $\Delta P_{si}$, $P_{si0}$, $P_{si,\mathrm{ma}}$ and $P_{si,\mathrm{mi}}$ are the power variation within $\Delta t$, initial power, maximum power and minimum power of the *ith* SG bus, respectively. $R_{si\mathrm{d}}$ and $R_{si\mathrm{u}}$ are the landslide and climbing speed limits of the *ith* SG bus, respectively.

REG usually adopts maximum power point tracking control and the maximum power is determined by

natural conditions. Thus, the power output of REG cannot be increased but can be reduced rapidly within tens of milliseconds [3]. However, the PRS of a SG is much smaller than that of REG, so in only adjusting the power of a SG it can be hard to stabilize the unbalanced power when overload occurs. The PRS of REG is restricted by the capacity and PRS of the SG. The power regulation capability of REG is modeled as:

$$\Delta P_{wk} \geq R_{\mathrm{wkd}} \Delta t \text{ and } \Delta P_{wk} > P_{wk,\min} - P_{wk0} \tag{2}$$

where $\Delta P_{wk}$, $P_{wk0}$ and $P_{wk,\min}$ are the power variation within $\Delta t$, initial power, and minimum power of the *kth* REG bus, respectively, and $R_{\mathrm{wk}d}$ is the landslide speed limit of the *kth* REG bus, which meets:

$$\sum_{k=1}^{n_{wr}} R_{\mathrm{wkd}} = \max\left\{0, R_{\Sigma \mathrm{su}} - R_{\Sigma sd}\right\} \tag{3}$$

where $n_{wr}$ is the quantity of adopted REG buses.

The real-time line flow is determined by the initial power, mutation power caused by shedding and the continuous variation power under regulation, given as:

$$P_L = P_{L0} - P_{Lu} - \nu_p \Delta t \tag{4}$$

where $P_{L0}$ and $P_{Lu}$ are the initial and mutation power of the line, respectively, and $\nu_P$ is the integrated PRS of SG and REG to the line.

The continuous variation power depends on the integrated PRS and regulation times of the SG and REG, whereas the mutation power is determined by the shedding power of the SG. The mutation power and integrated PRS are also affected by the active power sensitivity (APS) between the active power of the bus and the overload line as [21]:

$$\begin{cases} P_{Lu} = \sum\limits_{\mathrm{i}=1}^{n_{st}} H_{si} P_{sti} + \sum\limits_{j=1}^{n_{Bt}} H_{Bj} P_{Btj} \\ \nu_p = \sum\limits_{i=1}^{n_{sr}} R_{\mathrm{s}i} H_{si} + \sum\limits_{k=1}^{n_{wr}} R_{wk} H_{wk} \end{cases} \tag{5}$$

where $H_{si}$, $H_{Bj}$ and $H_{wk}$ are the APS of the *ith* SG bus, *jth* load bus and *kth* REG bus, respectively. $n_{st}$ and $n_{Bt}$ are the quantities of SG and load buses adopted for shedding, respectively, while $n_{sr}$ and $n_{wr}$ are the quantities of the SG buses adopted for regulation, respectively. $P_{sti}$ and $P_{Btj}$ are the respective shedding power of the *ith* SG bus and *jth* load bus. $R_{si}$ and $R_{wk}$ are the PRS of the *ith* SG bus and *kth* REG bus, respectively.

The initial power has a certain value, while the shedding power is directly proportional to the power mutation. Therefore, the shedding power can be reduced by increasing the integrated PRS. The PRS of a SG is related to the shedding position and amount, whereas the PRS of REG is limited by the capacity and position of the SG. Therefore, the shedding power can be reduced only by optimizing the shedding position and coordinating the amount of shedding power and PRS with full regard to security and economy.

## 3 Modeling of dynamic security domain

The line temperature depends on the real-time power [10]. The line flow continuously changes because of power regulation, and this causes variations in the speed of temperature rise and allowable overload time. The allowable overload time must be considered as a function of the shedding power and PRS, rather than a constant value as is the current practice. The variation of line flow determines the security condition of the line dynamic after the overload. Hence, the relationship among the initial power, integrated PRS, and mutation power characterizes the dynamic security domain of line under overload.

The heating power is mainly due to the effect of current, and the heat dissipation power includes convection heat dissipation between the line and the surrounding air and radiative heat dissipation. Active power has little effect on voltage because the line overload generally occurs in the transmission system. The radiation heat dissipation accounts for less than 10% of the total heat dissipation because of the limited difference between the line and environment temperatures. Therefore, the thermal balance equation can be expressed as [22]:

$$\frac{d\left(T_c - T_a\right)}{dt} + \frac{K_3}{K_1}\left(T_c - T_a\right) = -\frac{K_2}{K_1}\left(P_{L0} - P_{Lu} - \nu_P t\right)^2 + \frac{K_0}{K_1} \tag{6}$$

where $T_c$ and $T_a$ are the absolute temperatures of the line and environment, respectively. The parameters $K_0$, $K_1$, $K_2$, $K_3$ are given as:

$$\begin{cases} K_0 = \rho_L Q_{L0}^2 / \left(U_{L0}^2 \pi r_L^2\right) \\ K_1 = \nu_L \pi r_L^2 c_L \\ K_2 = \rho_L / \left(U_{L0}^2 \pi r_L^2\right) \\ K_3 = 2\pi r_L M_L + 8\pi r_L N_L T_a^3 \end{cases}$$

where $\rho_L$, $M_L$ and $N_L$ are the resistivity, convection heat dissipation coefficient and radiation heat dissipation coefficient, respectively. $Q_{L0}$ and $U_{L0}$ are the initial reactive power and voltage of the line, respectively. $\nu_L$, $r_L$ and $c_L$ are the density, radius and specific heat capacity of the line, respectively.

The line temperature can be solved by:

$$\begin{aligned} T_c = {} & B_1 \nu_P^2 t^2 - \left(2B_2 \nu_P^2 + 2B_1 \nu_P P'_{L0}\right) t + C e^{-B_4 t} + B_1 P'^2_{L0} \\ & + 2B_3 \nu_P^2 + 2B_2 \nu_P P'_{L0} + T_a + K_0 / K_3 \end{aligned} \tag{7}$$

where $P'_{L0} = P_{L0} - P_{Lu}$, and $C$ is obtained via the line temperature $T_0$ under normal operation as:

$$C = T_0 - T_a - B_1 P'^2_{L0} - 2B_3 v_P^2 - 2B_2 v_P P'_{L0} - K_0/K_3 \tag{8}$$

with the parameters $B_1$, $B_2$, $B_3$, $B_4$ given as:

$$\begin{cases} B_1 = K_2/K_3 \\ B_2 = K_2 K_1/K_3^2 \\ B_3 = K_2 K_1^2/K_3^3 \\ B_4 = K_3/K_1 \end{cases}$$

Given that the allowable overload time is presented in minutes, the term $o(t^2)$ in the Taylor expansion of $e^{-B_4 t}$ accounts for less than 5%. Therefore, Eq. (7) becomes a quadratic function of temperature and time after ignoring $o(t^2)$. If two moments are solved by (7) when the temperature is the maximum allowable temperature, then the temperature between the two moments must be greater than the maximum allowable temperature according to the curve feature of the upper parabolic quadratic function. Therefore, the unique solution or non-solution of (7) is an essential condition to guarantee the safety of the line, and can be expressed as:

$$\left[2B_2 v_P^2 + 2B_1 v_P P'_{L0} + B_4 C\right]^2 - \left(4B_1 v_P^2 + 2B_4^2 C\right)\Delta T_{0c} \le 0 \tag{9}$$

where $\Delta T_{0c} = T_0 - T_{c,\max}$ and $T_{c,\max}$ is the maximum allowable temperature.

The dynamic security domain under the shedding power and power regulation to solve $P_{Lu}$ based on (9) and $P'_{L0} = P_{L0} - P_{Lu}$ is expressed as:

$$\Delta P(v_p) + P_{Lu} \ge P_{L0} \tag{10}$$

where $\Delta P(v_p)$ is a variation obtained using:

$$\Delta P(v_p) = \frac{B_2\sqrt{4\left[B_1 v_p + \frac{1}{2}B_4^2 C\right]\Delta T_{0c}} - B_1 B_4\left[C + 2v_p\right]}{2B_1 B_2 v_p} \tag{11}$$

The dynamic security domain represents the safety of the overload line in the condition of line flow variation. The safe recovery of the overload line is determined by the initial power, mutation power, and integrated PRS. The dynamic security can be evaluated using (10) on the basis of the shedding power and integrated PRS under a certain initial power. The change of line flow in the dynamic security domain mainly includes two parts from (10): the power variation caused by the power regulation of SG and REG, which is negatively related to the integrated PRS, and the power variation caused by the generator tripping and load shedding, which is determined by the APS and the amount of shedding power.

## 4 Coordination control idea

### 4.1 Principle of minimum generator tripping

Line security is related to the shedding power and APS. The set of integrated PRS and shedding power that satisfy the dynamic security domain is obtained by substituting (5) into (10) as:

$$\Gamma_1 = \left\{ P(v_p) + \sum_{i=1}^{n_{st}} H_{si} P_{sti} + \sum_{j=1}^{n_{Bt}} H_{Bj} P_{Btj} \ge P_{L0} \right\} \tag{12}$$

Larger APS of the shedding bus requires more mutation power under the same shedding power from (5). Therefore, larger APS of the shedding bus results in less shedding power required to ensure the safe recovery under a certain integrated PRS according to (10). Giving $H_{s1}$ and $H_{s2}$ as the APS of the SG buses, $H_{b1}$ and $H_{b2}$ as the APS of the load buses, when $H_{s1} > H_{s2}$ and $H_{b1} > H_{b2}$, the relationships between the integrated PRS and shedding power are denoted by the solid lines in Fig. 1 according to (12) in the scenarios of $H_{s1}$ and $H_{b1}$, $H_{s1}$ and $H_{b2}$, $H_{s2}$ and $H_{b2}$.

The PRS of SG buses reduces after partial generator tripping, while the remaining SGs after shedding can only participate by reducing the power output because the power of the shedding buses demonstrates a positive relation with the power flow of the overload line. The set of the integrated PRS and shedding power based on (5) is expressed as:

$$\Gamma_2 = \left\{ v_p \le \sum_{i=1}^{n_{st}} \eta_{si} R_{sid} H_{si} + \sum_{k=1}^{n_{wr}} R_{wk} H_{wk} \right\} \tag{13}$$

where $\eta_{si} = P_{sti}/P_{si0}$.

Larger shedding power requires smaller integrated PRS. The shedding power in (13) demonstrates a linear

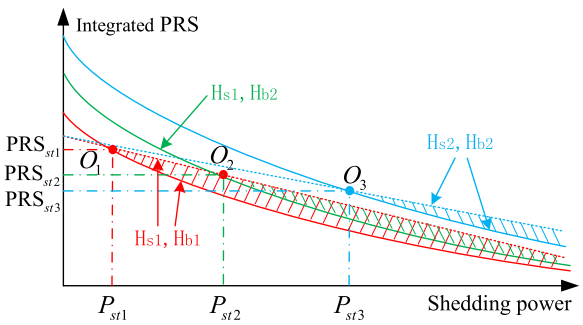


**Fig. 1** The set of shedding power

relationship with the integrated PRS and related to the APS of the SG bus. Large APS causes large integrated PRS under a certain shedding power. The dotted blue and red lines in Fig. 1 denote the relationship between the shedding power and integrated PRS in (13) when the APS is $H_{s1}$ and $H_{s2}$, respectively.

The generator tripping meeting the requirements of both (12) and (13) is the minimum amount of shedding power under a certain PRS. The line temperature rise can be decelerated by increasing the power mutation. Therefore, large APS of the SG bus reduces the generator tripping. $P_{st1}$, $P_{st2}$, and $P_{st3}$ are the minimum shedding power under the APS combinations of $\{H_{s1}, H_{b1}\}$, $\{H_{s1}, H_{b2}\}$ and $\{H_{s2}, H_{b2}\}$, respectively. The shedding power decreases with the increase of APS, and the integrated PRS of $O_1$, $O_2$ and $O_3$ continues to decrease (from (5)), as shown in Fig. 1.

The shedding power of each SG is equal to its normal power. Therefore, the shedding power of the SG bus is discontinuous. The safe recovery of the overload line can be realized when the shedding power is greater than or equal to the minimum shedding power. Therefore, the following optimal shedding power should be greater and the closest to the minimum shedding power:

$$\tilde{P}_{sti} = \sum_{m=1}^{n_{si}} \lambda_{mt,si} P_{m,si} \tag{14}$$

where $P_{m,si}$ is the normal power of a generator in the *ith* SG bus, and $n_{si}$ is the number of generators with different power output values in the *ith* SG bus. $\lambda_{mt,si}$ is the number of generators with power $P_{m,si}$, which can be expressed as:

$$\lambda_{mt,si} = \left\{ \lambda_{mt,si} \middle| \min \left( \sum_{m=1}^{n_{si}} \lambda_{mt,si} P_{m,si} - P_{oti} \right), \ \lambda_{mt,si} \in N_{m,si} \right\} \tag{15}$$

where $N_{m,si} = \{1, 2, \ldots n_{m,si}\}$, $n_{m,si}$ is the number of generators with power $P_{m,si}$ in the *ith* SG bus, and $P_{oti}$ is the minimum shedding power.

### 4.2 Coordination control principle

The integrated PRS reaches its maximum and generator tripping is at a minimum when all generators are regulated according to the climbing or landslide speed limit. However, at least one power source bus should be the balance bus. This uses different PRS values to balance the system power. The integrated PRS is at maximum if only one balance bus exists. The total PRS can be expressed as:

$$R_{sys} = \sum_{i=1}^{n_{sr}} R_{si} + \sum_{k=1}^{n_{wr}} R_{wk} \tag{16}$$

$R_{sys}$ should be zero to ensure system power balance. $R_{sys}$ is greater than zero when the PRS of the SG and REG buses are at the climbing speed limits, while the climbing speed of REG is zero. The balance bus can be determined by replacing the climbing speed limit with the landslide speed limit of each power source bus in the largest to smallest order of APS under this condition. If $R_{sys}$ is greater than 0 when the power source bus ranked $m-1$ is replaced and $R_{sys}$ is smaller than 0 when the power source bus ranked $m$ is replaced, then a PRS of the power source bus ranked $m$ must exist to make $R_{sys}$ equal to 0. The power source bus ranked $m$ can be used as the initial balance bus before generator tripping. The search ensures that only one balance bus exists and the remaining power source buses are regulated at the speed limit. The PRS can be expressed as follows when the bus ranked $m$ is the initial balance bus:

$$R_{Gm0} = \sum_{x=1}^{m-1} R_{Gxd} - \sum_{x=m+1}^{n_{Gr}} R_{Gxu} \tag{17}$$

where $n_{Gr} = n_{sr} + n_{wr}$, $R_{Gxd}$ and $R_{Gxu}$ are the respective landslide and climbing speed limits of bus ranked $x$.

$R_{sys}$ can reach zero when the PRS of the first-searched REG bus is replaced by the landslide speed limit according to (3) and (16). Therefore, the first-searched REG bus can work as the balance bus, and the initial integrated PRS can be obtained by substituting (17) into (5) as:

$$v_{p0} = \sum_{x=1}^{m-1} R_{Gxd} H_{Gx} + \sum_{x=m+1}^{n_{Gr}} R_{Gxu} H_{Gx} + R_{Gm0} H_{Gm} \tag{18}$$

where $H_{Gx}$ and $H_{Gm}$ are the APS of buses ranked $x$ and $m$, respectively.

The principle of the coordination control to block cascading failures includes three modules: dynamic security evaluation, minimum generator tripping point search and optimal control scheme of generator tripping and load shedding, as shown in Fig. 2. Dynamic security evaluation determines whether generator tripping is required. The dynamic security domain is modeled first using (10), and the SG, load, and all power source buses are then ranked according to the APS in descending order. The initial integrated PRS can be calculated using (18) to conduct the evaluation. Generator tripping and load shedding are avoided if the dynamic security domain is satisfied. The APS of power source buses is set according to the search of the initial

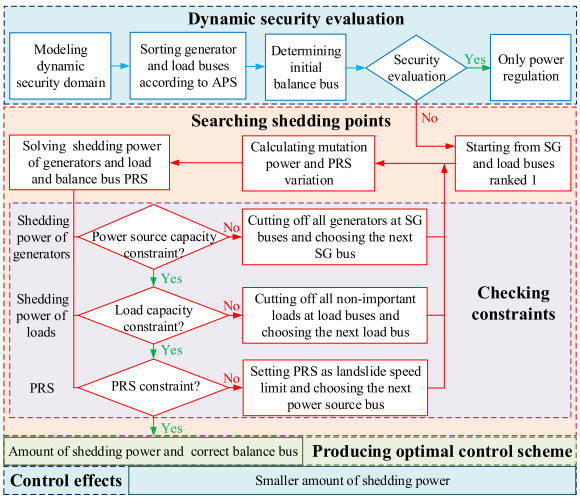


**Fig. 2** Principle of the coordination control to block cascading failures

balance bus. Otherwise, the shedding scheme should be searched according to the sort order of buses.

The PRS of the balance bus must be reduced after generator tripping because the landslide speed is reduced, while the generator tripping and load shedding should be equal to ensure the real-time power balance. If the shedding positions are the ranked 1 of SG and load bus, then the mutation power and variation of the integrated PRS after shedding can be expressed as:

$$\begin{cases} P_{Lu1} = P^{m}_{st1,B1}\left(H_{s1} - H_{B1}\right) \\ \Delta v_{p1} = \eta^{m}_{s1,B1} R_{s1}\left(H_{s1} - H_{Gm}\right) \end{cases} \tag{19}$$

where $P^{\mathrm{m}}_{st1,B1}$ is the shedding power of the SG bus ranked 1 when the power source bus ranked $m$ is the balance bus and load shedding is implemented on the load bus ranked 1. $H_{s1}$ and $H_{B1}$ are the APS of the SG and load buses ranked 1, respectively. $\eta^{\mathrm{m}}_{s1,B1} = P^{\mathrm{m}}_{st1,B1}/P_{s10}$ and $P_{s10}$ is the initial power.

The mutation power and variation of the integrated PRS are functions of $P^{\mathrm{m}}_{st1,B1}$. The shedding power required for safe recovery can be determined by substituting (5) and (19) into (10). However, the generator tripping must satisfy the constraint of power source capacity. The load shedding power determined by the generator tripping, which bears the constraint of load capacity, must be less than the permissible shedding power of the load bus. The required PRS of the balance bus is affected by the generator tripping, and hence generator tripping should obey the PRS constraint of the balance bus. $P^{\mathrm{m}}_{st1,B1}$ is the minimum shedding power if it satisfies these constraints. Otherwise, the next bus is searched. The shedding power $P^{\mathrm{m}}_{st2,B1}$ of the SG bus ranked 2 is calculated under the condition that all generators of SG bus ranked 1 are cut off when the constraint of power source capacity cannot be satisfied, i.e., $P^{k}_{st1,B1} > P_{s10}$. The shedding power $P^{\mathrm{m}}_{st1,B2}$ of the SG bus ranked 1 is recalculated under the condition that all non-important loads of the load bus ranked 1 are cut off when the constraint of load capacity is not satisfied, i.e., $P^{k}_{st1,B1} > P_{B10} - P_{B1,\min}$. $P_{B10}$ and $P_{B1,\min}$ are the initial and important loads of the load bus of the APS ranked 1. The shedding power $P^{\mathrm{m+1}}_{st1,B1}$ of the SG bus ranked 1 is recalculated under the condition that the PRS of the power source bus ranked $m$ is set as the landslide speed limit and the power source bus ranked $m+1$ works as the balance bus when the PRS constraint of the balance bus is not satisfied, i.e., $R_{Gm\mathrm{d}} \le \eta^{m}_{G1,B1} R_{G1} + R_{Gm0} \le R_{Gm\mathrm{u}}$.

All constraints should also be examined for $P^{\mathrm{m}}_{st2,B1}$, $P^{\mathrm{m}}_{st1,B2}$ and $P^{\mathrm{m+1}}_{st1,B1}$. If all constraints are satisfied, then the corresponding optimal shedding power can be obtained using (14). Otherwise, the search should be conducted in the same way until the calculated shedding power satisfies the constraints and the optimal control scheme can then be produced. A purpose of the optimal control scheme is to fully exploit the power control ability of the overload line and realize the minimum generator tripping under the premise of satisfying the need for safe operation of the line.

## 5 Producing algorithm for optimal control scheme

The shedding power of the SG bus ranked $\alpha$ is $P^{\beta}_{G\alpha,B\gamma}$ when the load shedding position is the load bus ranked $\gamma$, and the balance bus is the power source bus ranked $\beta$. All generators of SG buses ranked from 1 to $\alpha$ and all non-important loads of load buses ranked from 1 to $\gamma - 1$ should be cut off when $P^{\beta}_{G\alpha,B\gamma}$ cannot satisfy the constraint of power source capacity. The PRS of power source buses ranked from $m$ to $\beta - 1$ are set as landslide speed limits. According to (19), the amount of load shedding of bus ranked $\gamma$ and the PRS variation of the power source bus ranked $\beta$ can be expressed using the shedding power $P^{\beta}_{st(\alpha+1),B\gamma}$ of the SG bus ranked $\alpha + 1$ as:

$$\begin{cases} P_{Bt\gamma} = \sum\limits_{i=1}^{\alpha} P_{si0} + P^{\beta}_{st(\alpha+1),B\gamma} - \sum\limits_{j=1}^{\gamma-1} P_{Bja} \\ \Delta R_{G\beta} = \sum\limits_{i=1}^{\alpha} R_{si\mathrm{d}} + \eta^{\beta}_{st(\alpha+1),B\gamma} R_{s(\alpha+1)\mathrm{d}} - \sum\limits_{v=m+1}^{\beta-1} \Delta R_{Gv} - \Delta R_{Gk} \end{cases} \tag{20}$$

where $P_{Bja}$ is the maximum allowable shedding power of the $j^{th}$ load bus, $\eta^{\beta}_{st(\alpha+1),B\gamma} = P^{\beta}_{st(\alpha+1),B\gamma} \Big/ P_{s(\alpha+1)0}$, $\Delta R_{Gv} = R_{Gv\mathrm{d}} + R_{Gv\mathrm{u}}$ and $\Delta R_{Gk} = R_{Gk\mathrm{d}} + R_{Gk0}$.

Therefore, the mutation power and integrated PRS variation can be expressed as:

$$\begin{cases} P_{Lu} = \sum_{i=1}^{\alpha} P_{si0}H_{si} + P^{\beta}_{st(\alpha+1),B\gamma}H_{s(\alpha+1)} - \sum_{j=1}^{\gamma-1} P_{Bja}H_{Bj} - P_{Bt\gamma}H_{B\gamma} \\ \Delta v_p = \sum_{i=1}^{\alpha} R_{si\mathrm{d}}H_{si} + \eta^{\beta}_{st(\alpha+1),B\gamma}R_{s(\alpha+1)\mathrm{d}}H_{s(\alpha+1)} \\ \quad - \sum_{v=m+1}^{\beta-1} \Delta R_{Gv}H_{Gv} - \Delta R_{Gm}H_{Gm} - \Delta R_{G\beta}H_{G\beta} \end{cases} \tag{21}$$

$P^{\beta}_{st(\alpha+1),B\gamma}$ can be calculated by substituting (18) and (21) into (10). If all constraints are satisfied, the optimal control scheme can be generated as:

$$\begin{cases} T_s = \left\{ P_{s10}, \ldots, P_{s\alpha 0}, \tilde{P}^{\beta}_{st(\alpha+1),B\gamma} \right\} \\ T_B = \left\{ P_{B10}, P_{B20}, \ldots, \tilde{P}_{Bt\gamma} \right\} \\ T_R = \left\{ R_{G1d}, \ldots, R_{G(\beta-1)d}, R_{G\beta}, R_{G(\beta+1)u}, \ldots, R_{Gn_Gu} \right\} \end{cases} \tag{22}$$

where $T_s$ and $T_B$ are sets of buses and the amount of generator tripping and load shedding, respectively. $T_R$ is the PRS of power source buses, and $R_{G\beta}$ is the required PRS of the balance bus that can be obtained via (17). $\tilde{P}^{\beta}_{st(\alpha+1),B\gamma}$ is the optimal generator tripping determined by (21), and $\tilde{P}_{Bt\gamma}$ is the optimal load shedding obtained by (14) and $\tilde{P}^{\beta}_{st(\alpha+1),B\gamma}$.

All generators of SG buses ranked from 1 to $\alpha - 1$ and all non-important loads of load buses ranked from 1 to $\gamma$ should be cut off when $P^{\beta}_{G\alpha,B\gamma}$ cannot satisfy the constraint of load capacity. The PRS of power source buses from $m$ to $\beta - 1$ should be set as landslide speed limits. The mutation power and the integrated PRS can be expressed via the shedding power $P^{\beta}_{st\alpha,B(\gamma+1)}$ of the SG bus ranked $\alpha$ as:

$$\begin{cases} P_{Lu} = \sum_{i=1}^{\alpha-1} P_{si0}H_{si} + P^{\beta}_{st\alpha,B(\gamma+1)}H_{s\alpha} - \sum_{j=1}^{\gamma} P_{Bja}H_{Bj} - P_{Bt(\gamma+1)}H_{B(\gamma+1)} \\ \Delta v_p = \sum_{i=1}^{\alpha-1} R_{si\mathrm{d}}H_{si} + \eta^{\beta}_{st\alpha,B(\gamma+1)}R_{s\alpha\mathrm{d}}H_{s\alpha} \\ \quad - \sum_{y=m+1}^{\beta-1} \Delta R_{Gy}H_{Gy} - \Delta R_{Gm}H_{Gm} - \Delta R_{G\beta}H_{G\beta} \end{cases} \tag{23}$$

where $\Delta R_{G\beta}$ is the PRS variation of the power source bus ranked $\beta$, $P_{Bt(\gamma+1)}$ is the shedding power of load bus ranked $\gamma + 1$, and $\eta^{\beta}_{st\alpha,B(\gamma+1)} = P^{\beta}_{st\alpha,B(\gamma+1)} \Big/ P_{s\alpha 0}$.

$P^{\beta}_{st\alpha,B(\gamma+1)}$ can be calculated according to (10), (18) and (23). If all constraints are satisfied, the optimal control scheme is expressed as:

$$\begin{cases} T_s = \left\{ P_{G10}, P_{G20}, \ldots, \tilde{P}^{\beta}_{Gt\alpha,B(\gamma+1)} \right\} \\ T_B = \left\{ P_{B10}, P_{B20}, \ldots, P_{B\gamma 0}, \tilde{P}_{Bt(\gamma+1)} \right\} \\ T_R = \left\{ R_{G1d}, \ldots, R_{G(\beta-1)d}, R_{G\beta}, R_{G(\beta+1)u}, \ldots, R_{Gn_Gu} \right\} \end{cases} \tag{24}$$

where $\tilde{P}^{\beta}_{Gt\alpha,B(\gamma+1)}$ and $\tilde{P}_{Bt(\gamma+1)}$ are the optimal generator tripping and load shedding, respectively.

All generators of SG buses ranked from 1 to $\alpha - 1$ and all non-important load of APS load buses ranked from 1 to $\gamma - 1$ should be cut off when $P^{\beta}_{G\alpha,B\gamma}$ cannot satisfy the PRS constraint of the balance bus. The PRS of power source buses ranked from $m$ to $\beta$ should be set as landslide speed limits. The mutation power and the integrated PRS variation can be expressed by the shedding power $P^{\beta+1}_{st\alpha,B\gamma}$ of the SG bus ranked $\alpha$ when the power source bus ranked $\beta + 1$ works as the balance bus as:

$$\begin{cases} P_{Lu} = \sum_{i=1}^{\alpha-1} P_{si0}H_{si} + P^{\beta+1}_{st\alpha,B\gamma}H_{s\alpha} - \sum_{j=1}^{\gamma-1} P_{Bja}H_{Bj} - P_{B\gamma}H_{B\gamma} \\ \Delta v_p = \sum_{i=1}^{\alpha-1} R_{si\mathrm{d}}H_{si} + \eta^{\beta+1}_{st\alpha,B\gamma}R_{s\alpha\mathrm{d}}H_{s\alpha} \\ \quad - \sum_{y=m+1}^{\beta} \Delta R_{Gy}H_{Gy} - \Delta R_{Gm}H_{Gm} - \Delta R_{G(\beta+1)}H_{G(\beta+1)} \end{cases} \tag{25}$$

where $\Delta R_{G(\beta+1)}$ is the PRS variation of the generator ranked $\beta + 1$ and $\eta^{\beta+1}_{st\alpha,B\gamma} = P^{\beta+1}_{st\alpha,B\gamma} \Big/ P_{s\alpha 0}$.

The minimum shedding power $P^{\beta+1}_{st\alpha,B\gamma}$ can be calculated according to (10), (18) and (25). If all constraints are satisfied, the optimal control scheme can be expressed as:

$$\begin{cases} T_S=\left\{P_{G10},\ P_{G20},\ \ldots,P_{G(\alpha-1)0},\ \tilde{P}^{\beta+1}_{Gt\alpha,B\gamma}\right\} \\ T_B=\left\{P_{B10},\ P_{B20},\ \ldots,P_{B(\gamma-1)0},\ \tilde{P}_{Bt\gamma}\right\} \\ T_R=\left\{R_{G1d},\ \ldots,\ R_{G\beta d},\ R_{G(\beta+1)},\ R_{G(\beta+2)u},\ \ldots,\ R_{GnGu}\right\} \end{cases} \tag{26}$$

where $\tilde{P}^{\beta+1}_{Gt\alpha,B\gamma}$ and $\tilde{P}_{Bt\gamma}$ are the optimal generator tripping and load shedding, respectively.

## 6 Case studies

The IEEE 30-bus system shown in Fig. 3 is used to verify the correctness of the theoretical study. Buses 1, 2, 3, 5, 8, 14, 22, 23 and 27 are SG buses, and bus 13 is the REG bus with a capacity of 50 MVA. The capacity, climbing and landslide speed limits of SGs are listed in Table 1. Buses 10, 21, 24, 26, 29 and 30 are load buses, while all loads connected to buses 10, 21, 24, and 29 are important. The permissible shedding power of buses 26 and 30 are 11 MW and 10.5 MW, respectively. The initial line temperature, maximum allowable temperature, and permissible long-term power are 50 °C, 70 °C and 8.4 MW, respectively, while the ambient temperature is 30 °C. The normal power of SG buses 1, 2, 3, 5, 8, 14, 22, 23 and 27 are 63.62 MW, 9.68 MW, 10.47 MW, 10.73 MW, 10.77 MW, 12.36 MW, 21.59 MW, 19.2 MW and 26.91 MW, respectively. The normal power output of the REG bus is 37 MW.

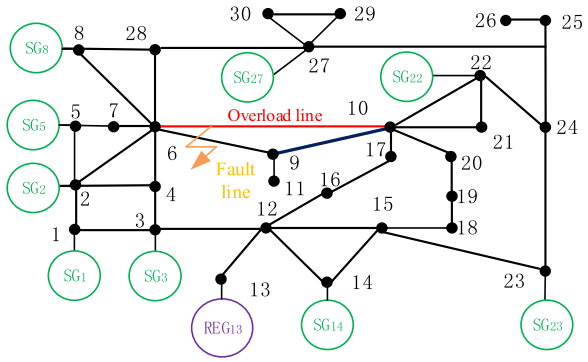


**Fig. 3** Simulation system

**Table 1** Parameters of the SGs

| Generation | Capacity (MVA) | L.C speed (MW/min) | L.L speed (MW/min) | Generation | Capacity (MVA) | L.C speed (MW/min) | L.L speed (MW/min) |
|---|---|---|---|---|---|---|---|
| $SG_1$ | 70 | 1.02 | 1.02 | $SG_{14}$ | 20 | 0.31 | 0.31 |
| $SG_2$ | 15 | 0.21 | 0.21 | $SG_{22}$ | 40 | 1.24 | 1.24 |
| $SG_3$ | 20 | 0.22 | 0.22 | $SG_{23}$ | 30 | 1.22 | 1.22 |
| $SG_5$ | 20 | 0.16 | 0.16 | $SG_{27}$ | 40 | 0.86 | 0.86 |
| $SG_8$ | 15 | 0.17 | 0.17 | $REG_{13}$ | 50 | −4.92 | 0 |

*L.C speed* Limit climbing speed, *L.L speed* Limit landslide speed

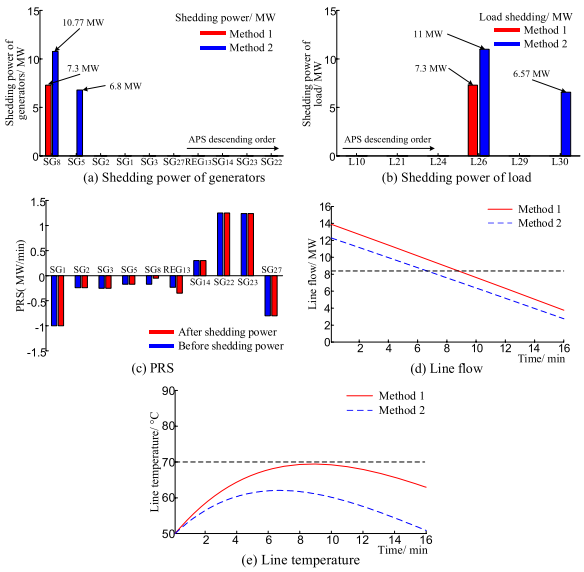


**Fig. 4** Control values and effects

The line tripping of $L_{6-9}$ occurs at $t=0$ which causes the power flow of $L_{6-10}$ to rise to 15.22 MW. Consequently, the line overload of $L_{6-10}$ occurs. The APS of each bus can be obtained by calculating the power flow. The APS sorting of the power source bus is: buses 8, 5, 2, 1, 3, 27, 13, 14, 23 and 22, while the APS sorting of the load bus is: buses 10, 21, 24, 26, 29 and 30. Bus 13 is the initial balance bus according to (16), and the integrated PRS is −0.72 MW/min based on (18). Therefore, the dynamic security domain is not satisfied with only power regulation based on (10).

### 6.1 Scenario 1: comparison of different methods

Method 1 is the proposed control method in this paper, and method 2 is the control method which calculates the amount of shedding power by only using the initial power flow of the overload line. The APS of the power source bus 8 is the largest, and the APS of the non-important load bus 26 is the largest. Therefore, the search starts from the power source bus 8 and the load bus 26. By substituting (5) and (19) into the dynamic security domain, it can be obtained that the required PRS of the balance bus is −0.35 MW/min, the minimum amount of generator tripping in method 1 is 7.3 MW, and so the load shedding of bus 26 is 7.3 MW. In comparison, the minimum amount of generator tripping in method 2 is 17.57 MW. According to the APS sequence, all generators at bus 8 are cut off, while 6.8 MW are cut off at bus 5. Therefore, load sheddings of 11 MW of bus 26 and 6.57 MW of bus 30 need to take place, as shown in Fig. 4a, b. According to (1) and (13), it can be judged that the amount of

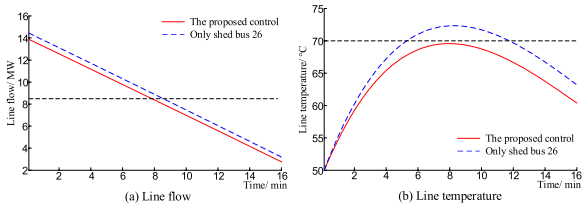


**Fig. 5** Control effects under load capacity constraint

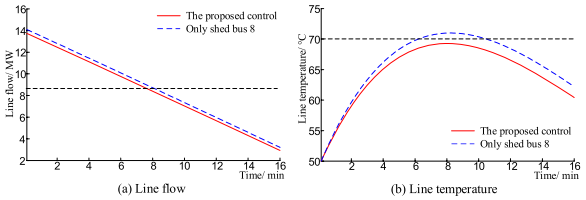


**Fig. 6** Control effects under power source capacity constraint

generator tripping and load shedding, and the PRS of balance bus, all meet the constraint conditions. Hence, the feasible amounts of generator tripping are 7.3 MW and 17.57 MW in methods 1 and 2, respectively.

After the implementation of methods 1 and 2, the PRS of bus 8 changes from − 0.17 to − 0.05 MW/min, the PRS of bus 13 changes from − 0.23 to − 0.35 MW/min, and the PRS of other buses remains basically unchanged, as shown in Fig. 4c. The power flow and temperature of $L_{6-10}$ are shown in Fig. 4d, e respectively. As seen, when method 1 is adopted, the line flow of $L_{6-10}$ decreases from 15.22 to 13.80 MW after the shedding power, and then drops further below 8.4 MW after about 8.75 min, while the temperature reaches a maximum of 69.23 °C. When method 2 is adopted, the line flow decreases from 15.22 to 12.37 MW, and then decreases further to below 8.4 MW after about 6.65 min, with the maximum temperature reaching 61.8 °C. Therefore, the overload line can be recovered safely under both methods 1 and 2. However, the amount of generator tripping in method 2 is 140.7% more than that in method 1, making the margin between the maximum temperature and the maximum allowable temperature too large, which is not conducive to system stability and economy.

### 6.2 Scenario 2: verification of the proposed control method under load capacity constraint

The permissible shedding power of bus 26 is changed to 4 MW. The constraint of load capacity cannot be satisfied if the load shedding of bus 26 is still 7.3 MW. Therefore, the shedding power of SG bus 8 is recalculated as 8.6 MW by substituting (5) and (23) into the dynamic security domain. The shedding power of load bus 30 is 4.6 MW and the PRS of bus 13 is − 0.35 MW/min. According to (13), all constraints are satisfied, and hence, the optimal shedding power sets of generator and load are $\{P_{st8} = 8.6\text{MW}\}$ and $\{P_{Bt26} = 4\text{MW}, P_{Bt30} = 4.6\text{MW}\}$, respectively.

The solid red line in Fig. 5 denotes the effects of the proposed control scheme on line flow and line temperature. The power of bus 8 drops from 6.77 to 2.17 MW and the PRS of bus 13 changes from − 0.29 to − 0.35 MW/min. The line flow of $L_{6-10}$ recovers to 8.4 MW at 8.0 min and the maximum temperature is 69.56 °C, as seen from Fig. 5a, b. In comparison, if only the permissible shedding power of bus 26 is cut off, as shown by the blue dotted line in Fig. 5, the line temperature reaches 70 °C at 5.4 min and then continues to rise. Hence, the overload line is recovered safely under the proposed control scheme which considers the load capacity constraint.

### 6.3 Scenario 3: verification of the proposed control method under power source capacity constraint

The normal power of bus 8 is changed to 5.77 MW, and the original shedding power of 7.3 MW cannot satisfy the constraint of power source capacity. Therefore, the shedding power of SG bus 5 is calculated as 1.9 MW according to (21) and the dynamic security domain, the shedding power of load bus 26 is 7.67 MW, and the PRS of bus 13 is − 0.37 MW/min. Thus, all constraints are satisfied, and the optimal generator tripping and load shedding schemes are $\{P_{st8} = 5.77\text{MW}, P_{st5} = 1.9\text{MW}\}$ and $\{P_{Bt26} = 7.67\text{MW}\}$, respectively.

As shown in Fig. 6a, compared with only shedding all generators of bus 8, the line flow of $L_{6-10}$ decreases from 14.10 to 13.75 MW, which drops below 8.4 MW after 7.6 min under the proposed control scheme. The maximum temperature of the overload line is 69.56 °C as shown in Fig. 6b. Hence, the overload line can be recovered safely under the proposed control scheme which considers the power source capacity constraint. In comparison, the line temperature reaches 70.9 °C after 8.2 min when only shedding all generators of bus 8, which exceeds the maximum allowable temperature and may cause line tripping.

### 6.4 Scenario 4: verification of the proposed control method under PRS constraint

The landslide speed limit of buses 8 and 27 are changed to 0.45 and 0.99 MW/min, respectively. The initial balance bus is 27 based on (16). The shedding power of the SG bus 8 is 4.6 MW and the shedding power of the load bus 26 is 4.6 MW according to (5, 19) and the dynamic security domain. However, the required PRS of bus 27 is − 1.02 MW/min, and the PRS constraint of the balance bus cannot be satisfied according to (13). Hence, bus 13 is changed into the balance bus based on (16). The shedding

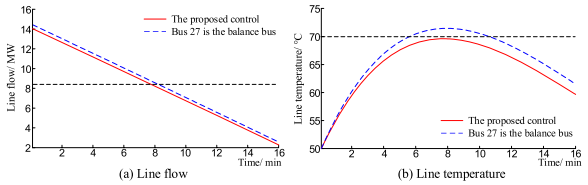


**Fig. 7** Control effects under PRS constraint

power of the SG bus 8 and load bus 26 are calculated as 6.1 MW according to (25) and the dynamic security domain. The required PRS of bus 13 is − 0.07 MW/min which meets the PRS constraint. $\{P_{st8,} = 6.1\text{MW}\}$ and $\{P_{Bt26} = 6.1\text{MW}\}$ are the optimal shedding schemes.

As shown in Fig. 7, the blue dotted lines denote the effects when bus 27 is the balance bus and the PRS of which is set to the landslide speed limit. The line temperature exceeds 70 °C after 5.7 min, and the overload line cannot be recovered safely. When the proposed control scheme is adopted, the PRS of bus 8 is changed from − 0.27 to − 0.20 MW/min, and the PRS of bus 13 is changed from 0 to − 0.07 MW/min. The line flow recovers to 8.4 MW at 7.8 min, and the maximum temperature is 69.60 °C as shown in the solid red line in Fig. 7. The proposed control scheme ensures the safe recovery of the overload line considering the PRS constraint.

## 7 Conclusion

The power flow of the overload line can be reduced by coordination of generator tripping, load shedding and the power regulation of REG and SG, so as to avoid the activation of overload protection and to block cascading failures. In this paper, by characterizing the power regulation capability of the overload line, the dynamic security domain that takes account of the change of line flow is established. Considering the constraints of load capacity, power source capacity and bus PRS, a cascading failure blocking method and producing algorithm for the optimal control scheme coordinated by SG and REG are proposed. The proposed method realizes the minimum generator tripping and load shedding for the safe and effective recovery of the overload line, effectively blocks the occurrence of the overload-dominated cascading failures, and ensures the safe and economic operation of the power system. The dynamic security domain is different from the existing line security domain in terms of meaning, content and effect, and can also be used for line N−1 static security assessment, critical line identification, line dynamic capacity increase, overload control improvement and other applications. In addition, the proposed method can provide a reference for the cooperative control of power source and load in a renewable energy dominated power system.

### Abbreviations

| | |
|---|---|
| REG | Renewable energy generation |
| SG | Synchronous generator |
| PRS | Power regulation speed |
| APS | Active power sensitivity |

### Acknowledgements

Not applicable.

### Author contributions

JO: Conceptualization, methodology, software, investigation, writing—original draft, supervision. JY: Validation, formal analysis, visualization, software, writing—original draft. XL: Investigation, writing: review and editing. YD: Writing: review and editing. JW: Writing: review and editing. All authors read and approved the final manuscript.

### Authors' Information

Jinxin Ouyang (1984-): male, currently an associate professor at School of Electrical Engineering, Chongqing University, China. His research interests include analysis, protection and control of renewable energy integrated power system, active distribution network and application of power electronic technology in power system.
Jianfeng Yu (1994-): male, currently pursuing the Ph.D. degree at the School of Electrical Engineering, Chongqing University, China. His research interests include control and protection of wind power integrated power system.
Xiaoxuan Long (1995-):male, received the M.Sc. degree from the School of Electrical Engineering, Chongqing University, China. His research interests include control and protection of power system.
Yanbo Diao (1984-): female, currently a professor at Chongqing City Management College, Chongqing, China. Her research interests include system simulation and big data analysis.
Jian Wang (1986-): male, currently an associate professor at School of Electrical Engineering, Chongqing University, China. His research interests include analysis, protection and control of renewable energy integrated power system, risk assessment of power system.

### Funding

This work was supported in part by the National Natural Science Foundation of China under Grant 51877018, in part by the Natural Science Foundation of Chongqing under Grant cstc2019jcyj-msxmX0321, in part by the Graduate Research and Innovation Foundation of Chongqing, China under Grant CYB22019.

### Availability of data and materials

Not applicable.

## Declarations

### Competing interests

The authors declare that they have no known competing financial interests or personal relationships that could have appeared to influence the work reported in this paper.

Received: 31 May 2022 Accepted: 3 March 2023
Published online: 26 March 2023

### References

1. Garcia, J. C., Wang, X., Xie, D. L., Zhao, Y., & Zuo, L. (2019). Control of communications-dependent cascading failures in power grids. *IEEE Transactions on Smart Grid, 10*(5), 5021–5031.

2. Liu, Y., Wang, Y., Yong, P., Zhang, N., Kang, C., & Lu, D. (2020). Fast power system cascading failure path searching with high wind power penetration. *IEEE Transactions on Sustainable Energy, 11*(4), 2274–2283.
3. Ouyang, J. X., Pang, M. Y., Li, M. Y., Zheng, D., Tang, T., & Wang, W. (2021). Frequency control method based on the dynamic deloading of DFIGs for power systems with high-proportion wind energy. *International Journal of Electrical Power & Energy Systems, 128*, 106764.
4. Bozorg, M., Bracale, A., Caramia, P., Carpinelli, G., Carpita, M., & De Falco, P. (2020). Bayesian bootstrap quantile regression for probabilistic photovoltaic power forecasting. *Protection and Control of Modern Power Systems, 5*(3), 36–47.
5. Ouyang, X., Yu, J. F., Pang, M. Y., & Diao, Y. B. (2022). An improved control method of fault ride-through for DPMWT-based wind farm considering coupling effect of HVDC transmission system. *International Journal of Electrical Power & Energy Systems, 141*, 108064.
6. Ouyang, J. X., Long, X. X., Du, X., et al. (2019). Voltage control method for active distribution network based on regional power coordination. *Energies, 12*(22), 4364.
7. Athari, M. H., & Wang, Z. (2018). Impacts of wind power uncertainty on grid vulnerability to cascading overload failures. *IEEE Transactions on Sustainable Energy, 9*(1), 128–137.
8. Zhang, X., Zhan, C., & Tse, C. K. (2017). Modeling the dynamics of cascading failures in power systems. *IEEE Journal on Emerging and Selected Topics in Circuits and Systems, 7*(2), 192–204.
9. Gan, G. X., Geng, G. C., Gao, B., et al. (2020). Blocking control of power system cascading failures considering line outages probability. *Power System Technology, 44*(1), 266–272.
10. Hu, J., Wang, J., Xiong, X. F., et al. (2020). An overload control strategy for AC/DC hybrid power grid considering dynamic electro-thermal characteristics of transmission lines. *Power System Protection and Control, 48*(7), 66–75.
11. Dong, X. J., Yang, H., Liu, P., et al. (2016). Criterion of accident overload and emergency control. *Power System Protection and Control, 44*(21), 165–169.
12. Staszewski, Ł, & Rebizant, W. (2018). DLR-supported overcurrent line protection for blackout prevention. *Electric Power Systems Research, 155*, 104–110.
13. Song, P., Xu, Z., Dong, H. F., et al. (2017). UPFC-based line overload control for power system security enhancement. *IET Generation, Transmission and Distribution, 11*(13), 3310–3317.
14. Cong, Y., Regulski, P., Wall, P., et al. (2016). On the use of dynamic thermal-line ratings for improving operational tripping schemes. *IEEE Transactions on Power Delivery, 31*(4), 1891–1900.
15. Zhang, Y. Q., Bansal, M., & Escobedo, A. R. (2020). Risk-neutral and risk averse transmission switch for load shed recovery with uncertain renewable generation and demand. *IET Generation, Transmission and Distribution, 14*(21), 4936–4945.
16. Jiao, Z. B., Ma, F., & Li, Z. B. (2019). Study on combined operation of gas-electricity coupling system and emergency overload control considering the characteristics of natural gas. *Proceedings of the CSEE, 39*(S1), 77–83.
17. Wei, B., Marzàbal, A., Perez, J., Pinyol, R., Guerrero, J. M., & Vásquez, J. C. (2019). Overload and short-circuit protection strategy for voltage source inverter-based UPS. *IEEE Transactions on Power Electronics, 34*(11), 11371–11382.
18. Ouyang, J. X., Yu, J. F., & Long, X. X. (2022). Adaptive overload protection method considering the dynamic thermal characteristics of a transmission line. *Power System Protection and Control, 50*(7), 40–48.
19. Zhou, Z. X., Wang, X. G., Du, D. X., et al. (2013). A coordination strategy between relay protection and stability control under overload conditions. *Proceedings of the CSEE, 33*(28), 146–153.
20. Wang, H. Y., Zhang, B. H., Yang, S. H., et al. (2016). Combined emergency control strategy of generator tripping and load shedding based on the characteristics of state plane. *Proceedings of the CSEE, 36*(15), 4144–4152.
21. Yue, X. L., Wang, T., Gu, X. P., et al. (2017). Control strategy for line overload based on sensitivity and power flow entropy. *Power System Protection and Control, 45*(21), 58–66.
22. Hu, J., Wang, J., Xiong, X., & Chen, J. (2019). A post-contingency power flow control strategy for AC/DC hybrid power grid considering the dynamic electrothermal effects of transmission lines. *IEEE Access, 7*, 65288–65302.